Optics Communications 293 (2013) 155–159

Contents lists available at SciVerse ScienceDirect

Optics Communications

journal homepage: www.elsevier.com/locate/optcom

Folded slot resonator array with efficient terahertz transmission

Joong Wook Lee [a,*,1], Jin-Kyu Yang [b,1], Ik-Bu Sohn [a], Chul Kang [a], Chul-Sik Kee [a,c]

[a] Advanced Photonics Research Institute, Gwangju Institute of Science and Technology (GIST), Gwangju 500-712, Republic of Korea
[b] Department of Optical Engineering, Kongju National University, Kongju 314-701, Republic of Korea
[c] Center for Subwavelength Optics, Seoul 151-747, Republic of Korea

ARTICLE INFO

Article history:
Received 20 June 2012
Received in revised form
27 November 2012
Accepted 27 November 2012
Available online 21 December 2012

Keywords:
Surface waves
Apertures
Optics of metals
Terahertz spectroscopy

ABSTRACT

We investigated transmission characteristics of folded slot resonators on a free-standing thin stainless steel film in terahertz frequency. The transmission at the resonance determined by the length of the slot was roughly proportional to the cosine function of the angle between directions of the slot and the polarization of incident light. Generally, the transmission at the resonance in the folded slot resonators was higher than that of a straight slot. Especially, the transmission efficiency at the 60° angle in the folded slot was three times higher than that in the straight slot. This is caused by strong oscillations of the accumulated charges inside the internal area formed by two arms of the folded slot. This finding demonstrates a new method for designing compact structures based on the folded geometry and for realizing THz devices.

1. Introduction

Tremendous attention has been focused on the subwavelength metallic structures, after the discovery of extraordinary optical transmission of light [1,2]. Resonant behaviors of electromagnetic waves through the plasmonic subwavelength geometries have been extensively studied owing to their fundamental importance and fascinating applications in various fields [3–5]. It is generally acknowledged that the resonant behaviors are primarily attributed to the resonant excitation of surface plasmon polaritons (SPPs) originated from the coupling of light to surface charge oscillation at the interface between metals and dielectrics [6–10]. Recently, the significant role of localized surface plasmons (LSPs) associated with the guided modes supported by the structural geometry has been well explored in the plasmonic subwavelength structures with various aperture shapes [11–16].

As the understanding has grown, methods to improve the efficiency in surface plasmon behaviors such as the resonant transmission and the strong near-field confinement of light have been suggested. Experimental results have been demonstrated that an extremely narrow metallic nanoslit leads to an enormous field enhancement as well as the optimized structure for the maximum transmission by controlling the structural shapes and arrangements of apertures [17,18]. Particularly, the resonances of the LSPs in a narrow slit and a hole were explained by a Fabry-Perot-like behavior due to the slit thickness and a fundamental mode due to the hole length, respectively [5,19]. Understanding the characteristics of the simple structures is important for realizing the promising devices which can substantially improve the performance and functionality, such as the propagation of the light with phase discontinuities, with appropriately designed structures to control the electromagnetic response [20]. As a direction to proceed the research, it is important to systematically investigate the transmission properties through the slightly modified structures of a narrow slot and its underlying physics.

In this paper, we present experimental and numerical studies of the efficient coupling of terahertz (THz) radiation to the LSPs in the folded slot resonator arrays, where the folding angles are changed from 0° to 90°. The results show that the transmission decreases with the increase of the folding angle. However, comparing with the peak value of the transmission at the straight slot resonators with the same length of the folded slot, the transmission in the folded slot resonators is enhanced over the folding angle of interest and even over three-fold at the folding angle of 60°. The numerical simulations show that the electric-charge current density and the electric near-field distribution reveal the strong field enhancement at the corner of the folded slots. Based on the folded slots which enable a design of compact plasmonic structure, a frequency-switchable THz filter is additionally investigated. This finding supports a simple idea for realizing a compact plasmonic structure for the design of plasmonic circuits or compact THz devices.

* Corresponding author. Tel.: +82 62 715 3447; fax: +82 62 715 3359.
E-mail addresses: leejujc@gist.ac.kr (J.W. Lee), jinkyuyang@kongju.ac.kr (J.-K. Yang).

[1] Joong Wook Lee and Jin-Kyu Yang contributed equally to this work.

0030-4018/$ - see front matter
http://dx.doi.org/10.1016/j.optcom.2012.11.099

2. Experiments and simulations

The proposed structures consist of a periodic arrangement of folded slots with the structural parameters depicted in Fig. 1(a). The sample area is 2 cm by 2 cm where 1450 apertures on a rectangular lattice are arranged with the periods of $P_x = 400\ \mu m$ and $P_y = 700\ \mu m$ in the x- and y-direction, respectively. The sample area is large enough to pass the THz beam with the diameter of about 2 mm without any loss, and thus any collective behavior in the structure is well captured. The plane of the sample is normal to the propagation direction of the incident THz waves. Note that the polarization of the incident THz wave is set to be along the x-direction that is parallel to the symmetric axis of the slot apertures where the resonance frequency is primarily determined by the equation, $f_c = c/2l$, where l is the total length of the slots. The samples were fabricated by using a femtosecond laser machining method, which is based on laser ablation performed by amplified femtosecond pulses. The microscopic images of a part of the fabricated samples are shown in Fig. 1(b). The 3σ standard deviation values of the line edge roughness (LER) of the perforated slots are roughly less than 5 μm. We are therefore sure that the structures are well-constructed since the LER values are up to two orders of magnitude less than the THz wavelengths of interest.

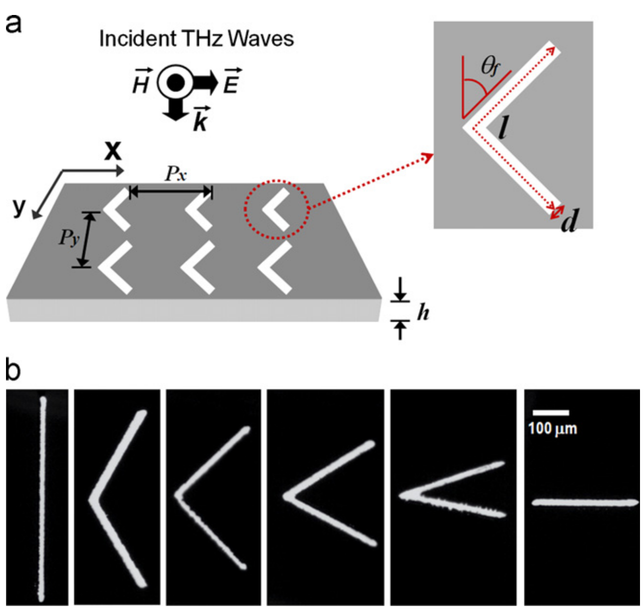

Fig. 1. (a) Experimental configuration for the THz transmission measurements of a folded slot resonator perforated on a free-standing stainless steel slab with the thickness h of 10 μm. The inset at the right defines the geometry of a unit cell. (b) Microscopic images of the folded slot resonators with different folding angles (θ_f) of 0°, 30°, 45°, 60°, 75°, and 90°.

In our experiments, we used a standard THz time-domain spectroscopy system with a spectral range from 50 GHz to 2 THz generated by a p-type InAs emitter [21,22]. The THz waves are detected by using a photoconductive antenna. The measured time traces are Fourier transformed to derive the frequency-domain spectra. The normalization is carried out simply over the entire frequency by dividing the spectral amplitude of the transmitted THz waves by one of the reference beams through a 2 cm by 2 cm reference blank cell. For simulations, we carried out a finite-difference time-domain (FDTD) method. Periodic boundary conditions are applied in the directions, x and y, in the structure plane and perfect matched layers are defined in z direction. Actually, the optical constants of stainless steel are large enough to regard it as a perfect metal in the THz range. So, in the FDTD simulations, we assumed that the complex dielectric constant of stainless steel is the same as that of aluminum extracted from Ref. [23] using the Drude model, where $\varepsilon_o = 4320$, $\omega_p = 1.73 \times 10^{16}$ Hz, and $\gamma = 6.93 \times 10^{13}$ Hz [24]. Zero-order transmission spectra and near electric-field and current density distributions in the sample surface were obtained by the numerical simulations.

3. Results and discussion

To characterize the THz property of the samples, the zero order transmission spectra were measured by illuminating the samples with the THz pulses at normal incidence, as shown in Fig. 2(a). The transmission measurements were carried out on the folded slot resonators with different folding angles of 0°, 30°, 45°, 60°, 75°, and 90°. Here, the folding angle θ_f is defined as the angle between one of the legs of a folded slot and the y-axis as shown in Fig. 1(a). In the case of a straight slot, the folding angle is therefore zero (the image on the very left in Fig. 1(b)) whereas the folding angle is 90° when the two arms of a folded slot are perfectly folded (the image on the very right in Fig. 1(b)). In a straight air slot at a perfect electric conductor, the cut-off frequency is

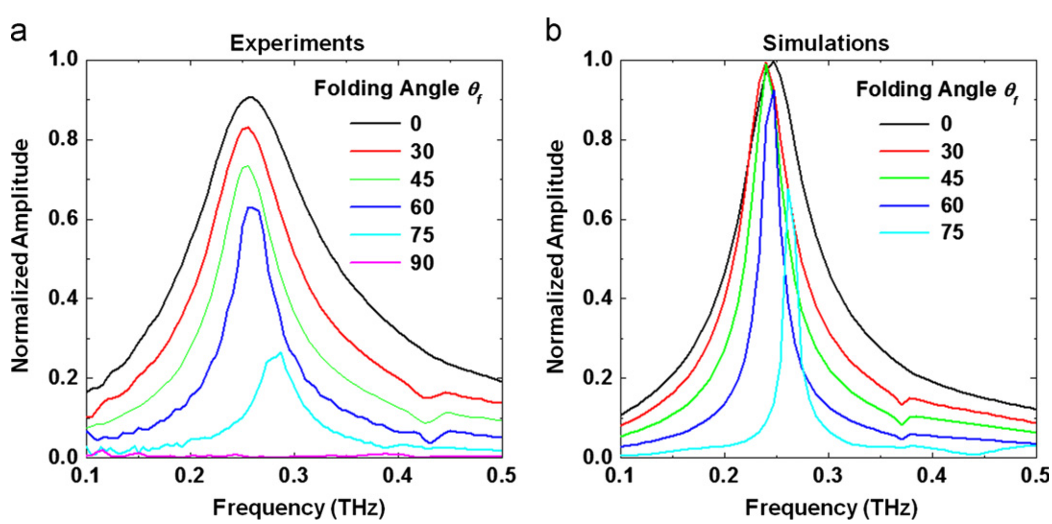

Fig. 2. (a) Measured THz transmission spectra of the folded slot resonators with different folding angles of 0°, 30°, 45°, 60°, 75°, and 90°. (b) Simulated THz transmission spectra of the folded slot resonators with different folding angles of 0°, 30°, 45°, 60°, and 75°.

determined by the equation, $f_c = c/2l = 0.25$ THz, where c denotes the speed of light in vacuum. In the experimental results, the peak transmission frequency was found at 0.26 THz, which agrees well with the fundamental cut-off mode of the slot waveguide. The peak frequency of THz transmission becomes large as the folding angle of the slots increases. According to the dispersion relation, transmission peak related with the diffraction by periodicity is located at the frequency of 0.75 THz, which is considerably far from the peaks of the resonant transmission [25,26]. This clarifies that the measured peaks are primarily attributed by resonant excitations of LSPs in the structures. The peaks of the measured transmission spectra are in reasonable agreement with ones of the simulated spectra as shown in Fig. 2. The discrepancy in the bandwidths of the resonant peaks may be attributed to a couple of reasons. The most important reason is that in simulation, the perfect plane wave was incident to the infinitely large film with an ideal folded slot array. However, in experiments, the incident THz waves were slightly focused and the sample may have inhomogeneity due to the imperfection of fabrication. Moreover, the width d of the fabricated slots was broader than what we expected. The simulations were obtained with the width of 25 μm, since the widths of the slots in the fabricated samples are roughly 25 μm.

For quantitative understanding of the folding effect on transmission efficiency, the peak values of the transmission spectra both in experiments and in simulations are indicated in Fig. 3 by the black squares and the red circles, respectively, as a function of the folding angle. In the case of the simulation results, we obtained the peak values from the Lorentzian fit. It is clear that the transmission decreases as the folding angle increases from 0° to 90°. However, the trend of the transmission variation is quite different in two regimes separated by around 60°. The peak values of transmission decrease slightly until 60° despite of the fact that the slot resonators are strongly folded. In contrast, the peaks rapidly decrease at the angle higher than 60°.

To understand the origin of the change of the transmission peak value at different folding angles, we use a simple expression to describe the transmission efficiency with the folding angle. It is well-known that the transmission amplitude is proportional to the sine function of the angle between the slot and the polarization of incident light. If the direction of the polarization is the y-axis as shown in the inset of Fig. 3, the transmitted amplitude is proportional to the $|\vec{E}|\cos\theta_f$, where $|\vec{E}|$ is the amplitude of

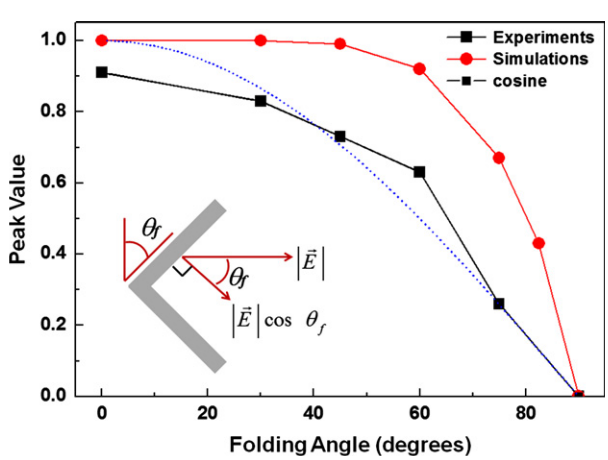

Fig. 3. (a) Comparison of the peak values of measured (black squares) and simulated (red circles) transmission at each resonance frequency. The inset shows the geometry of a folded slot with the folding angle θ_f. (For interpretation of the references to color in this figure legend, the reader is referred to the web version of this article.)

incident light and θ_f is the folding angle. We therefore plotted a cosine curve as the blue dotted curve in Fig. 3. It is worth noting that, although the measured and simulated results partly show higher transmission comparing with the curve in the range of the folding angle from 40° to 70°, Fig. 3 reveals that the peak value of the resonant transmission is roughly proportional to $|\vec{E}|\cos\theta_f$.

In order to further elucidate the relationship between the resonant transmission and the geometry of the slot resonators, we performed numerical simulations to excite the resonant mode by normally incident continuous wave with the resonance frequency. Fig. 4 shows the cut view of E_x and E_y along the center of the stainless steel film, and the cut view of J_x and J_y distributions along the surface of the film at the resonant frequency with the folding angle of 0° and 75°, respectively. As shown in Fig. 4(a), the x-polarized incident THz waves force the charge to oscillate between the corners of the straight slot, which accumulates the charge at the edge of the slot. Therefore, the narrow gap in the slot acts as a strong capacitor which induces the LSPs to strongly confine the electric field along the ridges of the slot aperture. In contrast, for the 75°-folded slot resonator, J_x is very weak, but J_y appears on two folded arms of the slot resonator with the opposite direction of the motion on each arm, as shown in Fig. 4(e) and (f). This means that the charges oscillate between the inside and outside formed by two oblique arms of the folded slot resonator.

The concept of a "λ-zone" capacitance for plasmonic systems may provide an intuitive method for understanding the behaviors [18,27]. The λ-zone capacitor can be defined as a static local capacitor, which induces the surface current flow inside a confined area of a diameter equal to one resonant wavelength of the incident electromagnetic wave, the so-called λ-zone. This concept is particularly useful for explaining the enhanced transmission due to the LSPs. Here, with increasing the folding angle, we can expect that the transmission efficiency due to the slot resonator decreases since the area of the λ-zone which effectively interacts with the incident THz wave is reduced with the decrease of the area of the inside formed by two arms. The current density distribution along the x-axis, shown in Fig. 4(g), is also affected by the geometry of the folded slot resonator. In this case, the flow of the charges is restricted by the two oblique arms, which leads to a decrease in THz transmission.

In addition, we compared the transmission characteristics of the folded slot resonators with one of the straight slot resonator, to verify the advantages of the folded plasmonic structures. The black squares in Fig. 5 show the peak values of the resonance in THz transmission spectra of the samples with different folding angles. The red circles in Fig. 5 represent the peak values of the THz transmission spectra, measured by changing the polarization, in a straight slot resonator. Here, the overall length of the straight slot and the folded slots is 600 μm. In some respects, the two geometries are of the same type in that they have the same spectral properties such as the resonant frequency and the same condition in the angle between the polarization and the structure. The transmission in the folded slot resonator remains high and even at the angle of 60° the peak value of the folded slot resonator is about three times higher than one of the straight slot resonator. This is resulted from both charges accumulated at the corner of the folded slot and mutual charge oscillations induced in the two arms of the slot which are not collinear.

To show the functionality of the folded slot resonator, we measured the normalized polarization-dependent transmission amplitude spectra through the periodic arrays of the slots with the folding angle of 60°, as shown in Fig. 6. The transmission peaks appear at 0.26 and 0.4 THz at the incident polarization of 0° and 90°, respectively. These resonant frequencies are related to

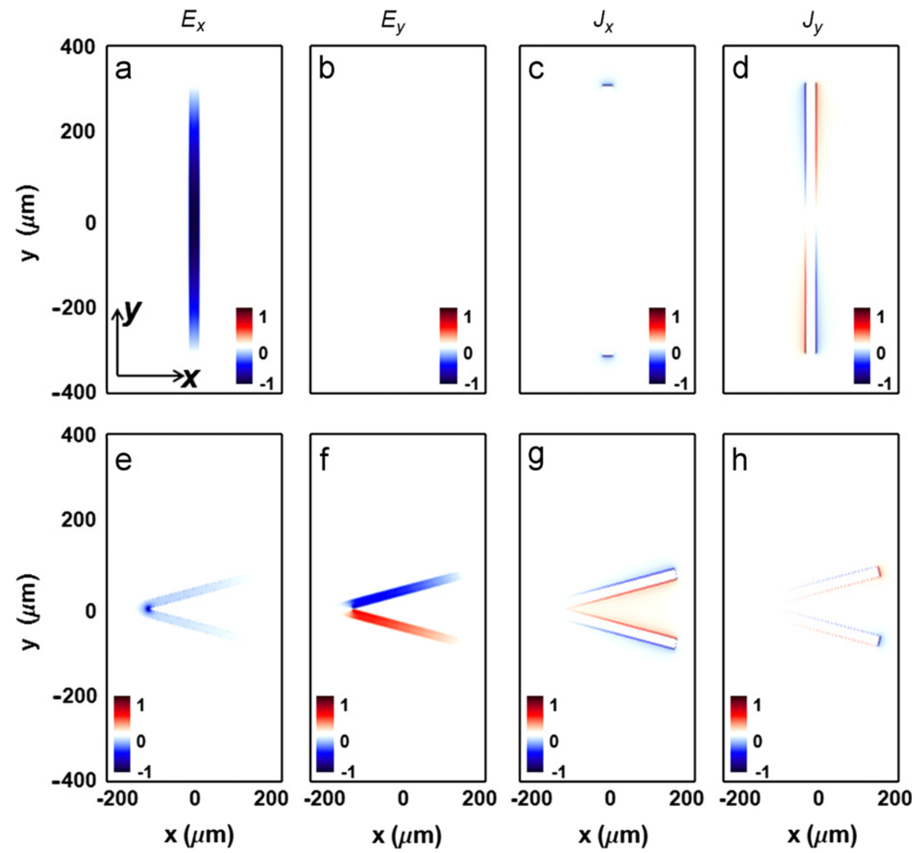

Fig. 4. (a)–(d) Simulation snapshots of E_x (a), E_y (b), J_x (c) and J_y (d) distributions of a slot with the folding angle of 0° in the xy plane of the sample. (e)–(h) Simulation snapshots of E_x (e), E_y (f), J_x (g) and J_y (h) distributions of a slot with the folding angle of 75° in the same plane presented in (a)–(d).

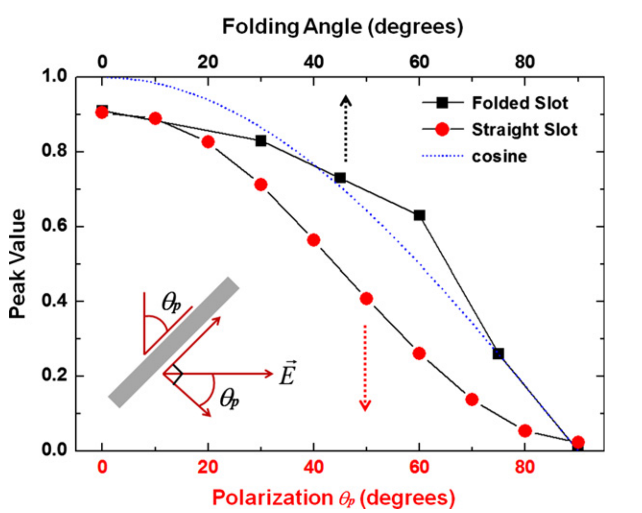

Fig. 5. Peak values of the resonant THz transmission versus the folding angle θ_f and the polarization θ_p. The black squares and red circles represent the results extracted from the experiments in Fig. 2(a) and the polarization-dependent THz transmission measurements in a straight slot resonator with the length of 600 μm (not shown here), respectively. (For interpretation of the references to color in this figure legend, the reader is referred to the web version of this article.)

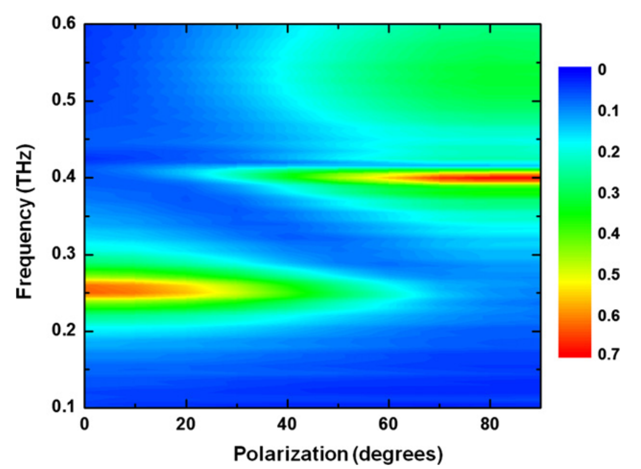

Fig. 6. Polarization-dependent transmission amplitude spectra of the periodic arrays of folded slot resonators with the folding angle of 60°. Two resonance frequencies of 0.26 and 0.4 THz appear at 0° and 90° polarization, respectively.

the total length of the slots and the length of one side (arm) of the folded slots, respectively. This demonstrates that the frequency-switchable THz filtering can be achieved by changing the incident THz polarization. In contrast, a straight slot resonator does not have any transmission peak at the incident polarization of 90° (not shown here). The folded slot structure will therefore play an important role in designing and realizing high-performance devices with high functionality and compact plasmonic structure.

4. Conclusion

In conclusion, we have studied both experimentally and theoretically the THz transmission characteristics of the folded slot resonators. The results showed that the resonant frequency of THz transmission is independent of the geometry of the folding structures, whereas the transmission efficiency decreases with the increase of the folding angle. According to the simulations and the polarization-dependent THz transmission measurements, even though the slot resonators become compact by folding their arms, the transmission efficiency remains high and even is three times higher than the peak value of the straight slot resonator. In addition, we showed that the devices with additional functionality such as frequency-switchable THz filtering can be realized. Our work may contribute to developing the devices requiring high sensitivity and high functionality over a broad range of the incident angle and to designing the geometry of compact plasmonic structures for THz devices.

Acknowledgment

This research was supported by Basic Science Research Program through the National Research Foundation of Korea (NRF) funded by the Ministry of Education, Science and Technology (2010-0021181 and 2010-0025701) and by the APRI Research Program of GIST.

References

[1] T.W. Ebbesen, H.J. Lezec, H.F. Ghaemi, T. Thio, P.A. Wolff, Nature 391 (1998) 667.
[2] W.L. Barnes, A. Dereux, T.W. Ebbesen, Nature 424 (2003) 824.
[3] J.A. Porto, F.J. García-Vidal, J.B. Pendry, Physical Review Letters 83 (1999) 2845.
[4] L. Martín-Moreno, F.J. García-Vidal, H.J. Lezec, K.M. Pellerin, T. Thio, J.B. Pendry, T.W. Ebbesen, Physical Review Letters 86 (2001) 1114.
[5] J.W. Lee, M.A. Seo, D.H. Kang, K.S. Khim, S.C. Jeoung, D.S. Kim, Physical Review Letters 99 (2007) 137401.
[6] S.A. Darmanyan, A.V. Zayats, Physical Review B 67 (2003) 035424.
[7] X. Fang, Z. Li, Y. Long, H. Wei, R. Liu, J. Ma, M. Kamran, H. Zhao, X. Han, B. Zhao, X. Qiu, Physical Review Letters 99 (2007) 066805.
[8] H.T. Liu, P. Lalanne, Nature 452 (2008) 728.
[9] J. Gómez Rivas, C. Schotsch, P.H. Bolivar, H. Kurz, Physical Review B 68 (2003) 201306.
[10] D. Qu, D. Grischkowsky, W. Zhang, Optics Letters 29 (2004) 896.
[11] A. Degiron, H.J. Lezec, N. Yamamoto, T.W. Ebbesen, Optics Communications 239 (2004) 61.
[12] K.J.K. Koerkamp, S. Enoch, F.B. Segerink, N.F. van Hulst, L. Kuipers, Physical Review Letters 92 (2004) 183901.
[13] J.B. Pendry, L. Martín-Moreno, F.J. García-Vidal, Science 305 (2004) 847.
[14] C.R. Williams, S.R. Andrews, S.A. Maier, A.I. Fernández-Domínguez, L. Martín-Moreno, F.J. García-Vidal, Nature Photon 2 (2007) 175.
[15] H. Cao, A. Nahata, Optics Express 12 (2004) 3664.
[16] J.W. Lee, M.A. Seo, D.J. Park, D.S. Kim, S.C. Jeoung, Ch. Lienau, Q.H. Park, P.C.M. Planken, Optics Express 14 (2006) 1253.
[17] M.A. Seo, H.R. Park, S.M. Koo, D.J. Park, J.H. Kang, O.K. Suwal, S.S. Choi, P.C.M. Planken, G.S. Park, N.K. Park, Q.H. Park, D.S. Kim, Nature Photon 3 (2009) 152.
[18] J.W. Lee, T.H. Park, P. Nordlander, D.M. Mittleman, Applied Physics Letters 97 (2010) 261112.
[19] Y. Takakura, Physical Review Letters 86 (2001) 5601.
[20] N. Yu, P. Genevet, M.A. Kats, F. Aieta, J.P. Tetienne, F. Capasso, Z. Gaburro, Science 334 (2011) 333.
[21] M. van Exter, D. Grischkowsky, Applied Physics Letters 56 (1990) 1694.
[22] Z. Jiang, M. Li, X.C. Zhang, Applied Physics Letters 76 (2000) 3221.
[23] D.Y. Smith, E. Shiles, M. Inokuti, in: E.D. Palik (Ed.), Handbook of Optical Constant of Solids, Academic, Orlando, Fla, 1985.
[24] Chul Jin-Kyu Yang, Ikbu Kang, Sohn, Chul-Sik Kee, Optics Express 18 (2010) 25371.
[25] H. Raether, Surface Plasmons on Smooth and Rough Surfaces and on Gratings, Springer-Verlag, Berlin, 1986.
[26] S.A. Maier, Plasmonics: Fundamentals and Applications, Springer, New York, 2007.
[27] J.H. Kang, D.S. Kim, Q.H. Park, Physical Review Letters 102 (2009) 093906.